Classical and Quantum Calculations for Short Stretched Chain Models

Dennis Perchak and Jerome H. Weiner*

Department of Physics and Division of Engineering, Brown University, Providence, Rhode Island 02912. *Received November 5, 1981*

ABSTRACT: The force–length–temperature relation for the freely rotating chain with up to six bonds is considered. Both rigid and flexible models are treated classically, and the flexible model is also analyzed from the quantum viewpoint.

I. Introduction

In a recent note[1] we showed that the force–length relation for a two-bond, freely jointed chain was radically different when based upon a rigid model in which fixed bond lengths are imposed as geometric constraints from that based upon a flexible model in which bond lengths are kept nearly constant by stiff linear springs.

We continue this study in this paper, considering short, stretched, freely rotating chains with up to six bonds, treating classically both rigid and flexible models and also considering the flexible model from the quantum viewpoint.

We will be concerned with the following questions: Does the behavior of rigid and flexible models continue to contrast as N increases? What is the difference in behavior between a strain ensemble, in which end-to-end length is imposed, and a stress ensemble, in which end force is imposed? What is the low-temperature behavior predicted by the quantum model and how rapidly does its high-temperature behavior approach the classical limit?

The plan of this paper is as follows: The analytical formulations used for the various models are summarized in section II. Numerical results are presented in section III with conclusions summarized in section IV. An Appendix presents further analytical and computational details.

II. Analytical Formulations

We provide in this section a summary of the analytical formulations which underlie the numerical results. In all cases we are dealing with a freely jointed chain with N bonds of bond length a. We treat the condition of both prescribed end-to-end vector $\mathbf{r}$ (strain ensemble) and prescribed applied force $\mathbf{f}$ (stress ensemble).

Strain Ensemble. As in ref 2, the atom positions with respect to a fixed rectangular Cartesian coordinate position are denoted by $\mathbf{x}_l$, $l = 0, 1, ..., N$, with $\mathbf{x}_0 = 0$. In ref 2 we regarded the Nth atom as free and introduced a curvilinear coordinate system for the $3N$-dimensional configuration space. Here we regard atom N as fixed at the prescribed displacement $\mathbf{x}_N = \mathbf{r}$ and introduce a curvilinear coordinate system q^i, $i = 1, ..., 3(N-1)$, for the remaining $3(N-1)$-dimensional configuration space. The definition of the curvilinear coordinate system used is given in the Appendix. The coordinates q^i are partitioned into two sets: soft variables q^α, $\alpha = 1, ..., f = 2N-3$, and hard variables q^A, $A = f+1, ..., 3(N-1)$, where $q^A = 0$ correspond to the equilibrium values of these variables in a flexible model and are identically zero in a rigid model.

Classical Flexible Model. The partition function Z_f for the classical flexible model takes the form

$$Z_f(r,T) = C(T) \int |g_{ij}|_0^{1/2} \prod_{\alpha=1}^{f} dq^\alpha \tag{1}$$

where

$$g_{ij} = \sum_{l=1}^{N-1} \frac{\partial \mathbf{x}_l}{\partial q^i} \cdot \frac{\partial \mathbf{x}_l}{\partial q^j} \tag{2}$$

is the covariant metric tensor of the q^i coordinate system, $|g_{ij}|_0$ is its determinant evaluated at $q^A = 0$, and the multiplying term $C(T)$ is independent of r.

Quantum Flexible Models. The partition function Z_{qu} for the quantum flexible model takes the form

$$Z_{qu}(r,T) = C'(T) \int Z_{h,qu} |g_{\alpha\beta}|_0^{1/2} \prod_{\alpha=1}^{f} dq^\alpha \tag{3}$$

where

$$Z_{h,qu}(q^\alpha,r,T) = \prod_{A=f+1}^{3(N-1)} \left[2 \sinh \left(\frac{\hbar \omega_A}{2kT} \right) \right]^{-1} \tag{4}$$

is the quantum partition function corresponding to the strong harmonic constraining potential $^1/_2 \kappa a_{AB} q^A q^B$ (see eq 9 of ref 2). The squared frequencies $\omega_A{}^2$ are obtained as eigenvalues of the matrix $(\kappa/m) g^{AB} a_{BC}$, where m is the atomic mass, $a_{AB} = \delta_{AB}$ for the freely jointed chain, and

$$g^{ij} = \sum_{l=1}^{N-1} \frac{\partial q^i}{\partial \mathbf{x}_l} \cdot \frac{\partial q^j}{\partial \mathbf{x}_l} \tag{5}$$

is the contravariant metric tensor.

It may be shown[3] that the high-temperature limit of Z_{qu} is Z_f.

Classical Rigid Model. The partition function Z_r for the rigid model takes the form

$$Z_r(r,T) = C'(T) \int |g_{\alpha\beta}|_0^{1/2} \prod_{\alpha=1}^{f} dq^\alpha \tag{6}$$

The force–length–temperature relation for the three models may be computed from the basic equation

$$f(r,T) = -kT \frac{\partial}{\partial r} \log Z(r,T) \tag{7}$$

However, for the classical flexible model it is more convenient to use eq 3 of ref 2, namely

$$f = -kT \frac{\partial}{\partial r} \log p \tag{8}$$

where $p(r) = p_{rw}(r)$ is the probability density for the end-to-end displacement $\mathbf{r}$ as computed on the basis of the random walk corresponding to a freely jointed chain with bond length a. The solution to this random walk problem is given by the well-known integral of Rayleigh. For small N, the following form due to Treloar[4] is more convenient:

$$p_N(r) = (8\pi r a^2)^{-1} N(N-1) \sum_{k=0}^{m} \frac{(-1)^k}{k!(N-k)!} \left[\frac{N - (r/a) - 2k}{2} \right]^{N-2} \tag{9}$$

where m is the integer in the interval

$$[(m - r/a)/2] - 1 \le m < (m - r/a)/2 \tag{10}$$

0024-9297/82/2215-0545$01.25/0

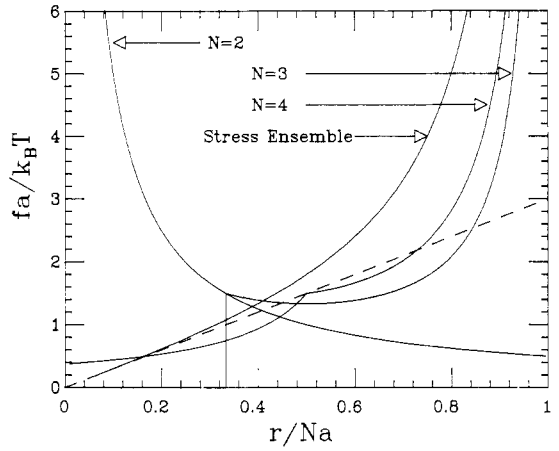

Figure 1. Force–displacement relation for the classical flexible model for N = 2–4, based on eq 8–10. Also shown is the stress ensemble result, eq 11. Dashed line represents force–displacement relation for a Gaussian chain.

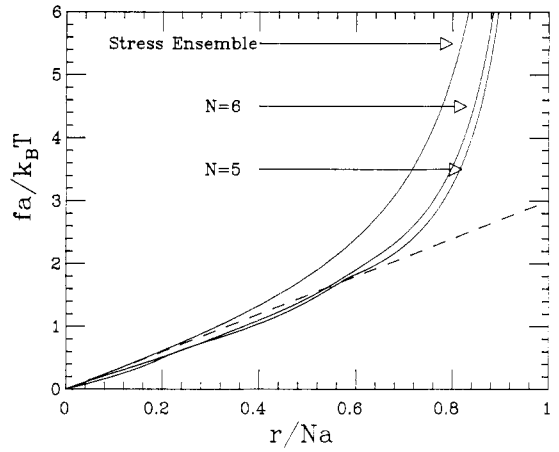

Figure 2. Force–displacement relation for the classical flexible model for N = 5 and 6, based on eq 8–10. Also shown is the stress ensemble result. Dashed line represents relation for a Gaussian chain.

with $p_N(r) = 0$ for $r > Na$.

Stress Ensemble. We treat only the classical flexible case for which the force–length–temperature relation is known:[5]

$$\frac{r}{Na} = \text{ctnh}\left(\frac{fa}{kT}\right) - \frac{kT}{fa} \qquad (11)$$

It is seen that if the intensive variable $r/(Na)$ is used as a measure of strain, then the stress ensemble leads to a size-independent stress–strain relation. Since it is expected that the stress and strain ensembles lead to the same relationship in the thermodynamic limit, as $N \to \infty$, eq 11 provides a useful measure of how rapidly the results for the classical flexible strain ensemble approach their limiting result.

III. Numerical Results

In this section we summarize the numerical results obtained.

(a) Classical Flexible Model. Figures 1 and 2 show the force–displacement relation for the strain ensemble for N = 2–6, based on eq 8–10, together with the stress ensemble result, eq 11. The anomalous result for N = 2 is the same as that obtained previously by other means in ref 1 and corroborated there by a Brownian dynamics computer simulation. For N = 3 and 4, the behavior is less surprising but remains somewhat counter to physical intuition, with zero force required in the interval $0 \le r/a < {}^1/_3$ for the case N = 3 and with a kink in the curve at $r/a = {}^1/_2$ for N = 4. Since it is difficult to give a physical basis for the discontinuity in the curve for N = 3 and the kink in the curve for N = 4, computer simulations of these cases by Brownian dynamics were performed. These are in agreement with these results, as shown in Figures 3 and 4. The behavior assumes a more expected form for N = 5 and 6 and, as seen from Figure 2, the approach to the limiting result of the stress ensemble appears to be reasonably rapid.

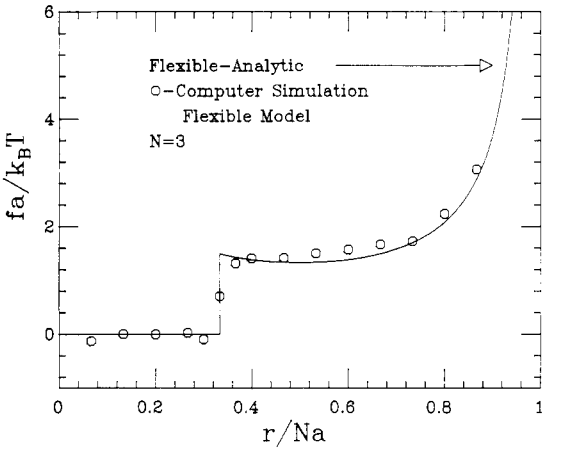

Figure 3. Force–displacement relation for N = 3 as given by Brownian dynamics simulation of the flexible model. Two computer runs were performed for each value of r used; the average of the two is plotted. The simulation employed a spring constant which leads to $\omega_0 = 1.34 \times 10^{14}$ s^{-1}. Also shown is the force–displacement relation calculated on the basis of eq 8–10.

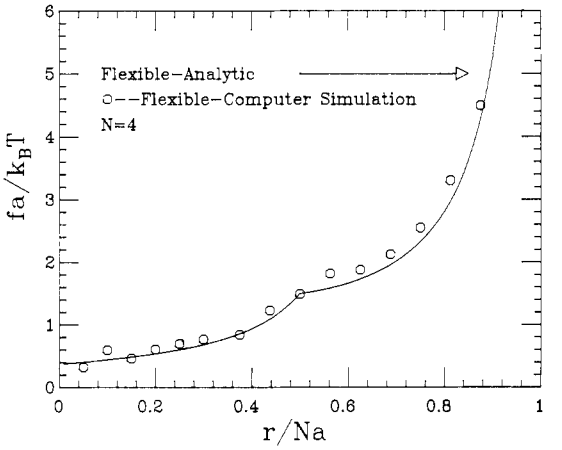

Figure 4. Force–displacement relation for N = 4 as given by Brownian dynamics simulation of the flexible model. In this case, only one computer run was performed for each value of r used. Also shown is the force–displacement relation calculated on the basis of eq 8–10.

(b) Classical Rigid Model. The rigid model for the case of N = 2 corresponds to Frenkel's governor model[6] and its simple analysis has been repeated in ref 1. For N > 2, calculations for the rigid model become difficult and have been carried out here, based on the numerical evaluation of eq 6 and 7, only for N = 3 and 4. Further details regarding the formulation of these problems will be found in the Appendix and in ref 7. The results are shown in Figures 5 and 6. Although for N = 2 the results for the classical flexible and rigid cases are completely different in character, as seen in Figure 3 of ref 1, the difference between the two, based on these limited results, appears to decrease with N and is already small for N = 4.

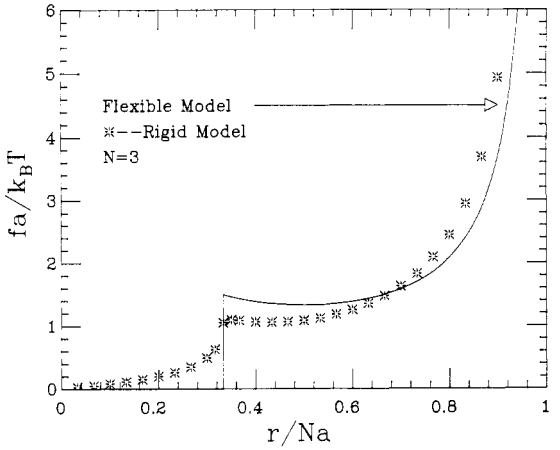

Figure 5. Force–displacement relation for the rigid model based on eq 6 and 7 evaluated numerically. Also shown is the corresponding flexible model relation based on eq 8–10.

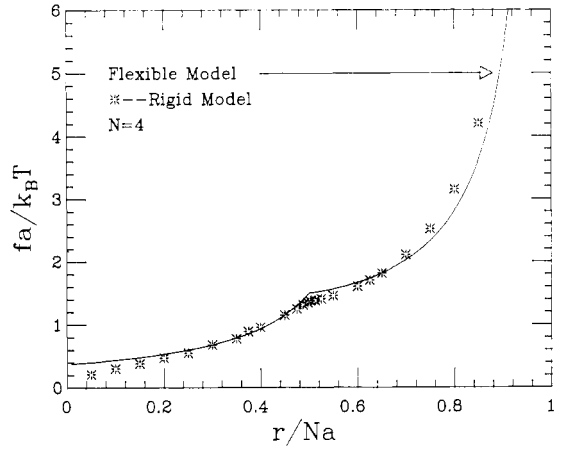

Figure 6. Force–displacement relation for the rigid model based on eq 6 and 7 evaluated numerically. Also shown is the corresponding flexible model relation based on eq 8–10.

(c) Quantum Flexible Model. For the case of $N = 2$ the quantum partition function of eq 3 may be evaluated analytically. The result is

$$Z_{qu}(r,T) = \frac{C(T)(a^2 - r^2/4)^{1/2}}{4 \sinh\left(\frac{\hbar\omega_2}{2kT}\right) \sinh\left(\frac{\hbar\omega_3}{2kT}\right)} \tag{12}$$

where

$$\omega_2 = 2^{-1/2}(r/a)\omega_0$$
$$\omega_3 = 2^{1/2}(\rho/a)\omega_0 \tag{13}$$

with

$$\omega_0 = (\kappa/m)^{1/2}$$
$$\rho = \tfrac{1}{2}(4a^2 - r^2)^{1/2} \tag{14}$$

Numerical results, with $\omega_0 = 1.3 \times 10^{14}$ s^{-1}, for the corresponding force–length relation are shown in Figure 7. The quantum results approach the classical results in the high-temperature limit as they should, with the two results almost equal at 300 K. The quantum results for low temperatures do not, however, approach the results for the rigid model. This is because the frequencies ω_2 and ω_3, and hence the zero-point energies, are r dependent.

The rapid approach of the quantum to the classical results at high temperatures is surprising since $\hbar\omega_0/kT$

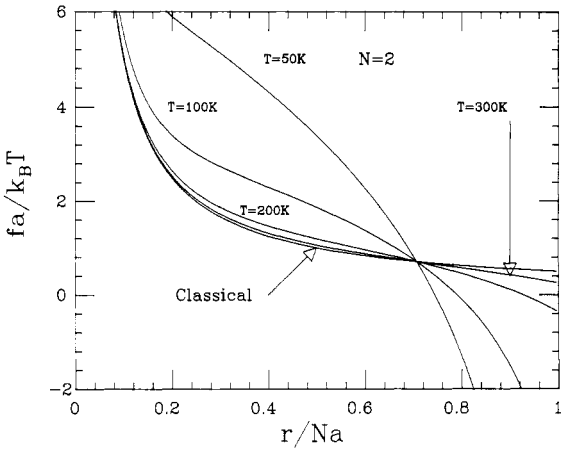

Figure 7. Force–displacement relation for the quantum flexible model for $N = 2$ as given by eq 7 and eq 12–14. Also shown is the relation for the 2-bond classical flexible model.

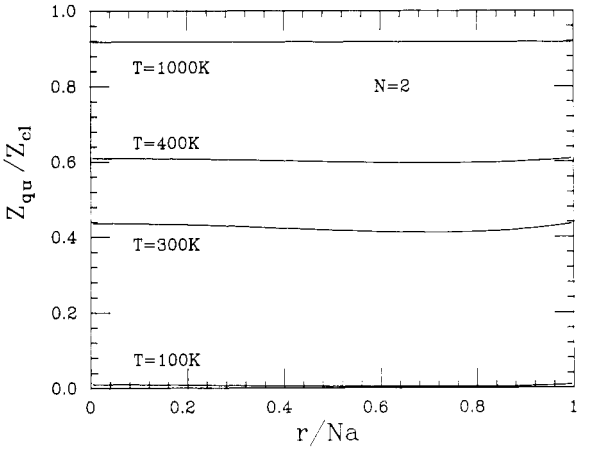

Figure 8. Ratio of quantum to classical partition functions for the 2-bond chain.

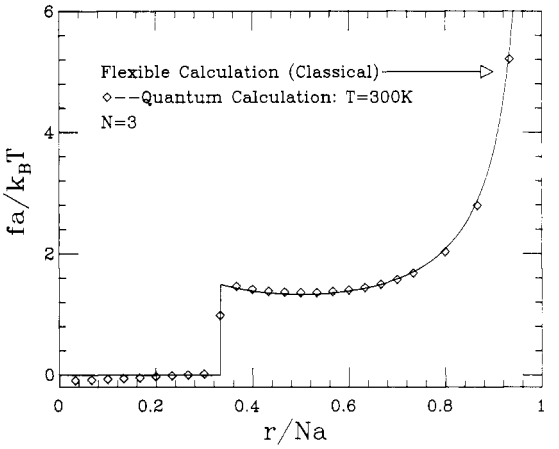

Figure 9. Force–displacement relation for the quantum flexible model for $N = 3$ based on eq 3, 4, and 7 evaluated numerically. $T = 300$ K and $\omega_0 = 1.34 \times 10^{14}$ s^{-1}. Also shown is the relation for the 3-bond classical flexible model.

~ 3 at $T = 300$ K. The result is clarified by Figure 8, where the ratio of quantum to classical partition functions is plotted. It is seen that at 300 K, the quantum effects are indeed large, with $Z_{qu}/Z_{cl} \sim 0.4$, but this ratio is nearly independent of r. Therefore quantum effects on the force–length relation at that temperature are negligible.

For $N > 2$, it was necessary to evaluate Z_{qu} and the resulting force–length relation numerically; only the cases $N = 3$ and 4 were considered. Results are shown in Figures 9–11. Again it is seen (Figure 10) that the low-temperature

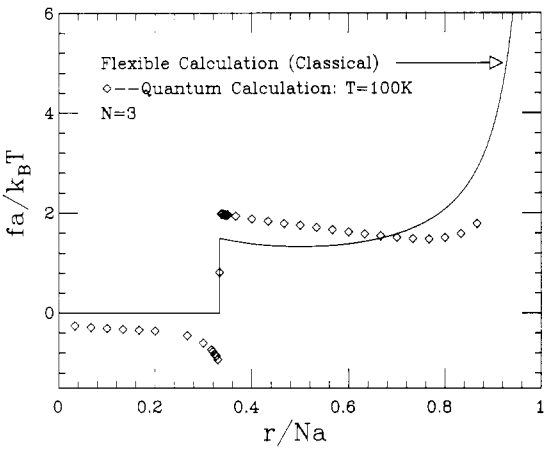

Figure 10. Force–displacement relation for the quantum flexible model for $N = 3$ with $T = 100$ K. Also shown is the relation for the 3-bond classical flexible model.

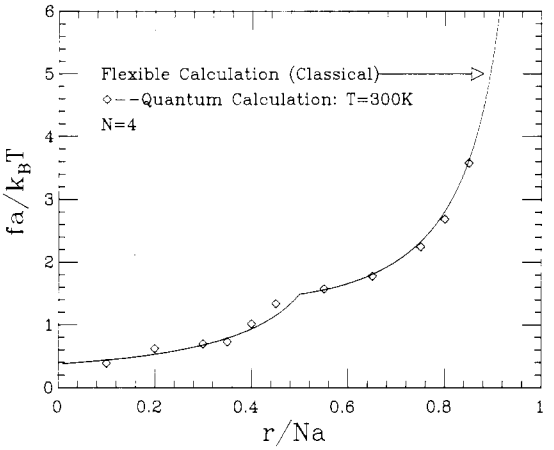

Figure 11. Force–displacement relation for the quantum flexible model for $N = 4$. $T = 300$ K and $\omega_3 = 1.34 \times 10^{14}$ s^{-1}. Also shown is the relation for the 4-bond classical flexible model.

behavior does not approach that for the rigid model while at high temperatures the classical flexible model behavior is approached, with the results quite close at $T = 300$ K.

IV. Conclusions

We have performed a limited number of calculations in the classical and quantum regimes for short, stretched, freely jointed chains. The results for the force–length relations may be summarized as follows:

In the classical regime, for the flexible model, the strain ensemble results approach, with increasing N, the length-independent stress ensemble result. The difference is reasonably small for $N = 6$, the largest value for which such computations were performed. Similarly, the difference in behavior between the rigid and flexible models decreases with increasing N and is already small for $N = 4$. The large difference between flexible and rigid models for $N = 2$, previously reported, appears to be an anomaly in this sequence.

In the quantum regime, the high-temperature behavior approaches that of the classical flexible model, in accordance with the general theory; the difference at room temperature is already quite small. The low-temperature behavior, for the cases studied, does not approach that of the classical rigid model because of the dependence of the zero-point energy upon the end-to-end length.

Because of the limited number of calculations on which they are based, we cannot ascribe a general character to these results. Further work on longer chains and on more realistic chain models is needed in order to determine their limits of validity.

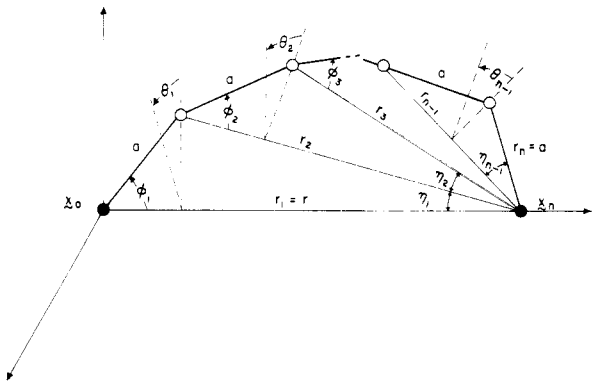

Figure 12. Definition of the curvilinear coordinate system.

Acknowledgment. This work has been supported by the Gas Research Institute (Grant No. 5080-363-0390) and by the National Science Foundation through the Materials Research Laboratory, Brown University.

Appendix

Let $\mathbf{x}_l$, $l = 0, 1, ..., N$, be the positions of the atoms with respect to a common rectangular Cartesian coordinate system, with $\mathbf{x}_0 = 0$ and $\mathbf{x}_N = \mathbf{r}$, the prescribed end-to-end displacement vector.

Define the vectors $\mathbf{r}_l = \mathbf{r} - \mathbf{x}_{l-1}$, $l = 1, ..., N$, the angles ϕ_l, between bond $\mathbf{x}_l - \mathbf{x}_{l-1}$ and $\mathbf{r}_l$, θ_l, rotation of atom l about $\mathbf{r}_l$, η_l, between $\mathbf{r}_{l+1}$ and $\mathbf{r}_l$, and γ_l, between bonds $\mathbf{x}_l - \mathbf{x}_{l-1}$ and $\mathbf{x}_{l+1} - \mathbf{x}_l$, for $l = 1, ..., N - 1$ (Figure 12), and the rotation matrices

$$\mathbf{R}_\theta^{(1)} = \begin{pmatrix} \cos\theta & 0 & -\sin\theta \\ 0 & 1 & 0 \\ \sin\theta & 0 & \cos\theta \end{pmatrix} \tag{A1}$$

$$\mathbf{R}_\theta^{(2)} = \begin{pmatrix} 1 & 0 & 0 \\ 0 & \cos\theta & \sin\theta \\ 0 & -\sin\theta & \cos\theta \end{pmatrix} \tag{A2}$$

Then

$$\mathbf{x}_1 = \mathbf{R}_{\theta_1}^{(1)} \begin{pmatrix} 0 \\ a\cos\phi_1 \\ a\sin\phi_1 \end{pmatrix} \tag{A3}$$

$$\mathbf{x}_l = \mathbf{R}_{\theta_1}^{(1)} \prod_{m=2}^{l} \mathbf{R}_{\eta_{m-1}}^{(2)} \mathbf{R}_{\theta_m}^{(1)} \begin{pmatrix} 0 \\ a\cos\phi_l - r_l \\ a\sin\phi_l \end{pmatrix} + r \qquad l = 2, \ldots, N-1 \tag{A4}$$

where $r_l = |\mathbf{r}_l|$.

The curvilinear coordinates q^i, $i = 1, ..., 3(N-1)$, may be defined in terms of these quantities as follows:

$$q^\alpha: \quad q^\alpha = \theta_\alpha, \quad \alpha = 1, ..., N-1$$
$$q^\alpha = \phi_\alpha - (N-1), \quad \alpha = N, ..., 2N-3 = f \tag{A5}$$

$$q^A: \quad q^A = |\mathbf{x}_{A-f} - \mathbf{x}_{A-f-1}| - a, \qquad A = f+1, ..., 3(N-1)$$

The matrix $\mathbf{g}^{AB}$ is tridiagonal and takes the form

$$\mathbf{g}^{AB} = \begin{pmatrix} 1 & -\cos\gamma_l & 0 & & \cdots & 0 \\ -\cos\gamma_l & 2 & -\cos\gamma_{l+1} & 0 & & 0 \\ 0 & -\cos\gamma_{l+1} & 2 & -\cos\gamma_{l+2} & & 0 \\ 0 & \cdots & 0 & -\cos\gamma_{N-1} & & 1 \end{pmatrix} \tag{A6}$$

The squared frequencies ω_A^2 are obtained from the eigenvalues of this matrix as described in the text. Details for $N = 3$ and 4 will be found in ref 7.

References and Notes

(1) Weiner, J. H.; Perchak, D. *Macromolecules* **1981**, *14*, 1590.
(2) Weiner, J. H., *Macromolecules*, preceding paper in this issue.
(3) Gō, N.; Scheraga, H. A. *Macromolecules* **1976**, *9*, 535.
(4) Flory, P. J. "Statistical Mechanics of Chain Molecules"; Interscience: New York, 1969; p 315.
(5) Volkenstein, M. V. "Configurational Statistics of Polymeric Chains" (translated from the Russian edition by S. N. Timasheff and M. J. Timasheff); Interscience: New York, 1963; p 450.
(6) Frenkel, J. "Kinetic Theory of Liquids"; Oxford University Press: London, 1946, Dover reprint, 1955; pp 474–476.
(7) Perchak, D. Doctoral Dissertation, Brown University, 1981.

Properties of Two-Dimensional Polymers

Jan Tobochnik and Itzhak Webman*

Department of Mathematics, Rutgers, The State University, New Brunswick, New Jersey 08903

Joel L. Lebowitz†

Institute for Advanced Study, Princeton, New Jersey 08540

M. H. Kalos

Courant Institute of Mathematical Sciences, New York University, New York, New York 10012.

Received August 3, 1981

ABSTRACT: We have performed a series of Monte Carlo simulations for a two-dimensional polymer chain with monomers interacting via a Lennard-Jones potential. An analysis of a mean field theory, based on approximating the free energy as the sum of an elastic part and a fluid part, shows that in two dimensions there is a sharp collapse transition, at $T = \Theta$, but that there is no ideal or quasi-ideal behavior at the transition as there is in three dimensions. The simulations and mean field theory agree very well. While the simulations are not sensitive enough to extract precise values for the exponent ν, it is clear that it is close to the Flory values: $\nu = {}^3/_4$, $T > \Theta$; $\nu = {}^1/_2$, $T < \Theta$. The mean field theory also gives $\nu = {}^2/_3$ at $T = \Theta$.

Introduction

The large-scale configurational properties of a polymer chain in a good solvent are determined by excluded volume interactions between distant segments of the chain, which cause the chain to swell relative to an ideal coil, where there are no interactions. In a poor solvent the net interaction between polymer segments is attractive, which causes the chain to contract relative to an ideal coil. These effects can be modeled by an effective interaction potential between polymer segments which has a strong short-range repulsive part and a weak attractive part. Then by varying the temperature, one can simulate the effects of a good solvent (high temperature) and a poor solvent (low temperature), just as in ordinary fluids where the repulsive part of the pair potential is most important at high temperatures and the attractive part is most important at low temperatures. In this work we shall use a truncated Lennard-Jones potential to represent the interaction between effectively independent polymer segments. Each segment then represents the average properties of many monomers.

Both theory and experiment indicate that in a good solvent the mean end-to-end distance of a polymer chain, R, depends on the number of polymer units, N, as $R = AN^\nu$, in the limit of large N. Here A is a constant that depends on the temperature or properties of the solvent. The exponent ν depends on the dimensionality of the system. Flory's theory[1] predicts that in three dimensions $\nu = 0.6$ and in two dimensions $\nu = 0.75$. Experiments, simulation studies, and other theories also give numbers for ν close to these.[2-4] These numbers reflect the more pronounced excluded volume effect in lower dimensions. In three dimensions a polymer segment can pass over or under another segment, but in two dimensions it is energetically unfavorable for two segments to cross.

In a poor solvent the polymer will confine itself to as small a region of space as is consistent with the excluded volume interaction. Assuming the density within this region is roughly uniform, then $N \propto R^d$, where d is the dimension of the system. Thus, we expect the power law dependence of the size of the chain R on the number of units N to be described by an exponent $\nu = 1/d$. For an ideal coil the power law dependence also holds with $\nu = {}^1/_2$. Thus, in three dimensions the size of the polymer is a smaller power of N than the ideal coil, while in two dimensions the exponent ν is the same for the ideal coil and the collapsed coil. The "collapse" of a polymer in two dimensions may therefore be qualitatively different from that observed in three dimensions.

Monte Carlo simulations in three dimensions show that the change in R as the temperature is lowered near the collapse transition becomes steeper with increasing N.[5] This suggests that for very long chains the collapse occurs over a very narrow temperature range. Experiments by Sun et al. indeed show this kind of phase transition for dilute solutions of polystyrene macromolecules in a cyclohexane solvent.[6] Recently, Vilanove and Rondelez[7] have measured the surface pressure for two-dimensional polymer chains and found values of ν given by 0.79 ± 0.01 and 0.56 ± 0.01, respectively, for two different polymer solutions. The first value is close to the Flory value predicted theoretically for swollen chains and the second is more typical of a collapsed chain. If the error bars quoted are

*Current address: Exxon Research and Engineering, Linden, N.J. 07036.
†Permanent address: Departments of Mathematics and Physics, Rutgers, The State University, New Brunswick, N.J. 08903.

0024-9297/82/2215-0549$01.25/0